NUMERICAL ANALYSIS OF STEADY FREE CONVECTION PAST OVER VERTICAL PLATE

Ahmed Ali Shaker
College of Engineering
Al-Qadisiya University

Mohamed Fadhil Thabit
College of Engineering
Al-Qadisiya University

Abstract

In this work a boundary layer analysis for free convection flow of viscous, incompressible fluid past over vertical plate is presented. A computer program is developed in Quick basic language to obtain numerical solutions for the resulting governing equations (mass, energy, and momentum). A parametric study of all involved parameters is conducted and a representative set of numerical results for the velocity profile and temperature distribution are illustrated graphically and physical aspects of the problem are discussed. The validity of results is verified and shows that there is a good agreement between the results of the present numerical solution and the correlation related to it.

التحليل العددي لانتقال الحرارة المستقر بشكل حر عبر صفيحة عمودية

أحمد علي شاكر
كلية الهندسة
جامعة القادسية

محمد فاضل ثابت
كلية الهندسة
جامعة القادسية

الخلاصة

في هذا البحث تم دراسة الحمل الحراري الحر لمائع لزج غير قابل للانضغاط يمر على سطح عمودي. تم إعداد برنامج بلغة (بيسك) لحل المعادلات الحاكمة(حفظ الكتلة،حفظ الطاقة وحفظ الزخم). يتم في هذا البرنامج حساب توزيع السرعة ودرجات الحرارة و تم مناقشة النتائج التي تم الحصول عليها من خلال المنحنيات والجداول لتوضيح اثر العديد من المتغيرات. وقد أعطت هذه الدراسة تقارب كبير مقارنةً بالنتائج العملية والنظرية لعدد من الباحثين.

Nomenclature

Symbol	
h	Heat Transfer Coefficient (W/m^2K)
Gr	Grashoff Number
k	Thermal Conductivity (W/mK)
L	Characteristic Length in the X direction
n	Number of Grid Nodes in the Vertical Direction
Nu	Nusselt Number
Nu_x	Local Nusselt Number
Pr	Prandtl Number
q	Heat Transfer Rate (W)

Re	Reynolds Number
T	Temperature
c_p	Specific Heat at Constant Pressure (*J/kg.K)*
u	Velocity in Axial Direction (*m/s)*
U	Dimensionless Velocity in Axial Direction
v	Velocity in Vertical Direction (*m/s)*
V	Dimensionless Velocity in Vertical Direction
X	Dimensionless Axial Direction of the Plate
Δx	The Distance Between Two Nodal Points in the Axial Direction (*m)*
ΔX	The Dimensionless Distance Between Two Nodal Points in the Axial Direction
y	Vertical Direction of the Plate (*m)*
Y	Dimensionless Vertical Direction of the Plate
Δy	The Distance Between Two Nodal Points in the Vertical Direction (*m)*
ΔY	The Dimensionless Distance Between Two Nodal Points in the Vertical Direction

Greek Symbols

Symbol	
ν	Kinematic Viscosity (m^2/s)
β	Thermal Coefficient of Volumetric Expansion (K^{-1})
μ	Dynamic Viscosity ($N.s/m^2$)
ρ	Density of Fluid (kg/m^3)
θ	Dimensionless Temperature

Subscripts

Symbol	
i	Refers to iteration
j,k	The Index Increment Along the Axial and Vertical Direction
w	Refers to Wall
∞	Fluid

Introduction

Free convection results when a fluid in the presence of gravity field undergoes density variations due to a uniform temperature distribution within the fluid. **Worster** and **Alison Leitch, 1985,** investigated the development of density stratification in a confined fluid due to a buoyancy source which gives rise to a vertical convective boundary layer. They find that the stratification is significantly different when the boundary layer is laminar rather than turbulent. In particular, the magnitude of the density gradient in the fluid interior increases rather than decreases in the direction of flow of the boundary layer, and this density gradient varies smoothly so that there is no density front between the stratified fluid and the unmodified homogeneous fluid. Laboratory experiments are described in which homogeneous fluid in a rectangular container was heated at a vertical sidewall. Vertical temperature profiles and streak photographs were taken which show the dominant features of the stratification mechanism under laminar flow conditions. They review similarity theory for a vertical, laminar, free-convection boundary layer in a homogeneous environment, and develop new similarity solutions for convective boundary layers in stratified environments. We use these analytic results to interpret qualitative features of the experimentally observed flow fields and to develop an expression for the depth of the stratified layer as a function of time. **Amable Y. Kurdyumov, V., 1988** investigates the effect of the buoyancy-induced laminar flow and temperature fields associated with a line source of heat in an unbounded environment are described by numerically solving the non-dimensional Bossiness equations with the appropriate boundary

conditions. The solution is given for values of the Prandtl number, the single parameter, ranging from zero to infinity. The far-field form of the solution is well known, including a self-similar thermal plume above the source. The analytical description close to the source involves constants that must be evaluated with the numerical solution. These constants are used when calculating the free convection heat transfer from wires (or cylinders of non-circular shape) at small Grashoff numbers. We find two regions in the flow field: an inner region, scaled with the radius of the wire, where the effects of convection can be neglected in first approximation, and an outer region where, also in first approximation, the flow and temperature fields are those due to a line source of heat. The cases of large and small Prandtl numbers are considered separately. There is good agreement between the Nusselt numbers given by the asymptotic analysis and by the numerical analysis, which we carry out for a wide range of Grashoff numbers, extending to very small values the range of existing numerical results; there is also agreement with the existing correlations of the experimental results. A correlation expression is proposed for the relation between the Nusselt and Grashoff numbers, based on the asymptotic forms of the relation for small and large Grashoff numbers. **Beithou, Albayrak, Abdulmajeed, 1998** present in their study, the variable porosity effects for a vertical plate in a variable porous medium. The governing partial nonlinear differential equations were transformed into a set of coupled ordinary differential equations, which was solved using the fourth-order Runge-Kutta method. The results obtained for the different power law index n, and variable porosity of the bed, were found to be in good agreement with previous studies. Results show that when porosity increases temperature variation becomes steeper, and the Nusselt number increases almost linearly with increasing porosity. **Singh and Ajay, 2003,** studied the two dimensional free convection and mass transfer flow of an incompressible, viscous and electrically conducting fluid past a continuously moving infinite vertical porous plate in the presence of heat source, thermal diffusion, large suction and under the influence of uniform magnetic field applied normal to the flow is studied. Usual similarity transformations are introduced to solve the momentum, energy and concentration equations. To obtain local similarity solutions of the problem, the similarity equations are solved using perturbation technique. The expressions for velocity field, temperature distribution, concentration field, drag coefficient, rate of heat, and mass transfer have been obtained. The results are discussed in detailed with the help of graphs and tables to observe the effect of various parameters. **Ayo, 2006** studied the effects of aspect ratio on the transient free convection generated by a heated vertical plate in a rectangular cavity for the characteristics and rates of heat transfer from the plate into the surrounding fluid medium. The plate is assumed to be an isothermal plate at a high temperature, suddenly immersed in air at a lower temperature inside the cavity whose walls are also assumed to be adiabatic. The rate of heat transfer by convection is found to increase with aspect ratio. At large times the temperature field stratifies and the heat transfer to the medium approached zero, the velocity field decaying gradually and the flow approaches its eventual quiescence. **Chaudhary 2006** investigated an exact solution of the unsteady free convection boundary-layer flow of an incompressible fluid past an infinite vertical plate with the flow generated by Newtonian heating and impulsive motion of the plate. The resulting governing equations are non-dimensional zed and their solutions were obtained in closed form with the help of Laplace-transform technique. A parametric study of all involved parameters was conducted and a representative set of numerical results for the velocity, temperature and skin-friction is illustrated graphically and physical aspects of the problem were discussed. The effect of Prandtl number on heat temperature may be analyzed he concluded that the thickness of thermal boundary layer is greater for air (Pr = 0.71) and there is more uniform temperature distribution across the thermal boundary layer as compared to water (Pr = 7.0) and electrolyte solution (Pr = 1.0). He observed that the increase of Prandtl number results in the decrease of temperature distribution. The reason is that smaller values of Prandtl number are equivalent to increasing thermal conductivity and therefore heat is able to diffuse away from the heated surface more rapidly than for higher values of Prandtl number. Thus temperature falls more rapidly for water than air and electrolyte solution. The maximum of the temperature occur in the vicinity of the plate and asymptotically approaches to zero in the free stream region.

Mathematical Model

In this study the Partial Differential Equations (PDE's) which describe the natural convection past over vertical heated plate are explained. The problem configuration considered is shown in **Figure (1).** The vertical plate is heated and the surrounding fluid is at rest. The vertical plate will be expressed in Cartesian Coordinates System with x direction taken parallel to plate and y direction normal to the plate. The following formulation is presented on the work of **Hornbeck, 1973** and **Incropera, 1996**.

Continuity Equation*:*

$$\frac{\partial(\rho.u)}{\partial x}+\frac{\partial(\rho.v)}{\partial y}=0 \qquad \textit{(1)}$$

For incompressible flow, ρ = constant and the continuity equation reduce to:

$$\frac{\partial u}{\partial x}+\frac{\partial v}{\partial y}=0 \qquad \textit{(2)}$$

X-momentum equation:

$$\rho.\left(u\frac{\partial u}{\partial x}+v\frac{\partial u}{\partial y}\right)=\frac{\partial}{\partial y}\left(\mu\frac{\partial u}{\partial y}\right)+\rho.g_x.\beta.(T-T_\infty) \qquad (3)$$

Energy equation:

$$\rho.c_p\left(u\frac{\partial T}{\partial x}+v\frac{\partial T}{\partial y}\right)=k\frac{\partial^2 T}{\partial y^2} \qquad (٤)$$

Boundary Conditions

The boundary conditions specified for the classical free convection problem are:

$$u(x,0)=0$$
$$u(x,\infty)=0$$
$$u(0,y)=0$$
$$v(x,0)=0$$
$$T(x,0)=T_w \qquad (5)$$
$$T(x,\infty)=T_\infty$$
$$T(0,y)=T_\infty$$

The Dimensionless Quantities

Before undertaking a numerical solution, the equations (2) to (4) and boundary conditions (5) may now be put in dimensionless form by the proper choice of variables. The variables chosen are those used by **Hornbeck, 1973**

$$\left.\begin{aligned} U &= \frac{v}{L^2.g_x.\beta(T-T\infty)}.u = \frac{uL}{v(Gr)} \\ V &= \frac{L.v}{v} \\ \theta &= \frac{T-T_\infty}{T_w-T_\infty} \\ X &= \frac{v^2}{g_x.\beta(T_w-T_\infty)L^4}.x = \frac{x}{L.(Gr)} \\ Y &= \frac{y}{L} \end{aligned}\right\} \quad (6)$$

Where $Gr = B.(T_w - T_\infty).L^3.g_x / v^2$ is the Grashoff number and g_x is the x-component of the acceleration due to gravity

Dimensionless Governing Equations

The dimensionless form is often more convenient to express the governing equations. It is developed to simplify the solution of many engineering problems and to avoid large quantities in calculation. When these variables are inserted into equations (2) to (4), the basic equations become in dimensionless form:

Continuity Equation*:*

$$\frac{\partial U}{\partial X} + \frac{\partial V}{\partial Y} = 0 \quad (7)$$

X-momentum equation:

$$U\frac{\partial U}{\partial X} + V\frac{\partial U}{\partial Y} = \frac{\partial^2 U}{\partial Y^2} + \theta \quad (8)$$

Energy equation:

$$U\frac{\partial\theta}{\partial X}+V\frac{\partial\theta}{\partial Y}=\frac{1}{\Pr}\frac{\partial^2\theta}{\partial Y^2} \tag{9}$$

Dimensionless Boundary Conditions

The boundary conditions in dimensionless form become:

$$\left.\begin{aligned} &U(X,0)=0\\ &U(X,\infty)=0\\ &U(0,Y)=0\\ &V(X,0)=0\\ &\theta(X,0)=1\\ &\theta(X,\infty)=0\\ &\theta(0,Y)=0 \end{aligned}\right\} \tag{10}$$

Numerical Analysis

The continuity, momentum, and energy equations which will be solved by using **Gauss-Elimination method**. The resulting algebraic forms for all equations presented in this work are solved by using a computer program written in QuickBasic language. The numerical formulation for Continuity, Momentum, and Energy equations are shown below respectively **Hornbeck, 1973**:

$$\frac{U_{j+1,k+1}^{(I+1)}-U_{j,k+1}}{\Delta X}+\frac{V_{j+1,k+1}^{(I+1)}-V_{j+1,k}^{(I+1)}}{\Delta Y}=0 \tag{11}$$

$$U_{j+1,k}^{(I)}\frac{U_{j+1,k}^{(I+1)}-U_{j,k}}{\Delta X}+V_{j+1,k}^{(I)}\frac{U_{j+1,k+1}^{(I+1)}-U_{j+1,k-1}^{(I+1)}}{2(\Delta Y)}=\frac{U_{j+1,k+1}^{(I+1)}-2U_{j+1,k}^{(I+1)}+U_{j+1,k-1}^{(I+1)}}{(\Delta Y)^2}+\theta_{j+1.k}^{(I)} \tag{12}$$

$$U_{j+1,k}^{(I+1)}\frac{\theta_{j+1,k}^{(I+1)}-\theta_{j,k}}{\Delta X}+V_{j+1,k}^{(I+1)}\frac{\theta_{j+1,k+1}^{(I+1)}-\theta_{j+1,k-1}^{(I+1)}}{2(\Delta Y)}=\frac{1}{\Pr}\frac{\theta_{j+1,k+1}^{(I+1)}-2\theta_{j+1,k}^{(I+1)}+\theta_{j+1,k-1}^{(I+1)}}{(\Delta Y)^2} \tag{13}$$

Where the subscripts (I) & (I+1) indicate values obtained in the (I)th & (I+1)th respectively. Equation (12) may be rewritten in a more useful form as:

$$\left[\frac{-1}{(\Delta Y)^2}-\frac{V^{(I)}_{j+1,k}}{2(\Delta Y)}\right].U^{(I+1)}_{j+1,k+1}+\left[\frac{2}{(\Delta Y)^2}+\frac{U^{(I)}_{j+1,k}}{(\Delta X)}\right].U^{(I+1)}_{j+1,k+1}+\left[\frac{-1}{(\Delta Y)^2}+\frac{V^{(I)}_{j+1,k}}{2(\Delta Y)}\right].U^{(I+1)}_{j+1,k}=\frac{U^{(I)}_{j+1,k}.U_{j,k}}{\Delta X}+\theta^{(I)}_{j+1,k} \tag{14}$$

Equation (14) written for k=1(1)n now constitutes n linear equations in the n unknowns $U^{(I+1)}_{j+1,k}$
The set of linear equations may be written in matrix form for momentum equation as follows;

$$\begin{vmatrix} \beta^{(I)}_1 & \Omega^{(I)}_1 & & & & & & \\ \alpha^{(I)}_2 & \beta^{(I)}_2 & \Omega^{(I)}_2 & & & & & \\ & \alpha^{(I)}_3 & \beta^{(I)}_3 & \Omega^{(I)}_3 & & & & \\ & & - & - & - & & & \\ & & & - & - & - & & \\ & & & & - & - & - & \\ & & & & & \alpha^{(I)}_{n-1} & \beta^{(I)}_{n-1} & \Omega^{(I)}_{n-1} \\ & & & & & & \alpha^{(I)}_n & \beta^{(I)}_n \end{vmatrix} \times \begin{vmatrix} U^{(i+1)}_{j+1,1} \\ U^{(i+1)}_{j+1,2} \\ U^{(i+1)}_{j+1,3} \\ - \\ - \\ - \\ U^{(i+1)}_{j+1,n-1} \\ U^{(i+1)}_{j+1,n} \end{vmatrix} = \begin{vmatrix} \Phi^{(I)}_1 \\ \Phi^{(I)}_2 \\ \Phi^{(I)}_3 \\ - \\ - \\ - \\ \Phi^{(I)}_{n-1} \\ \Phi^{(I)}_n \end{vmatrix} \tag{15}$$

Where

$$\alpha^{(I)}_k=-\frac{1}{(\Delta Y)^2}-\frac{V^{(I)}_{j+1,k}}{2(\Delta Y)} \qquad \beta^{(I)}_k=\frac{2}{(\Delta Y)^2}+\frac{U^{(I)}_{j+1,k}}{\Delta X}$$

$$\Phi^{(I)}_k=\frac{U^{(I)}_{j+1,k}.U_{j,k}}{\Delta X}+\theta^{(I)}_{j+1,k} \qquad \Omega^{(I)}_k=-\frac{1}{(\Delta Y)^2}+\frac{V^{(I)}_{j+1,k}}{2(\Delta Y)}$$

Equation (11) can be solved for $V^{(I+1)}_{j+1,k+1}$

$$V^{(I+1)}_{j+1,k+1}=V^{(I+1)}_{j+1,k}-\frac{\Delta Y}{\Delta X}\left(U^{(I+1)}_{j+1,k+1}-U_{j+1,k+1}\right) \tag{16}$$

Equation (13) may be rewritten in a more useful form as:

$$\left[\frac{-1}{(\mathrm{Pr})(\Delta Y)^2}-\frac{V^{(I+1)}_{j+1,k}}{2(\Delta Y)}\right].\theta^{(I+1)}_{j+1,k+1}+\left[\frac{2}{(\mathrm{Pr})(\Delta Y)^2}+\frac{U^{(I+1)}_{j+1,k}}{(\Delta X)}\right].\theta^{(I+1)}_{j+1,k+1}+$$
$$\left[\frac{-1}{(\mathrm{Pr})(\Delta Y)^2}+\frac{V^{(I+1)}_{j+1,k}}{2(\Delta Y)}\right].\theta^{(I+1)}_{j+1,k}=\frac{U^{(I+1)}_{j+1,k}}{\Delta X}.\theta_{j,k} \tag{17}$$

Equation (17) written for k=1(1)n now constitutes n linear equations in the n unknowns $\theta^{(I+1)}_{j+1,k}$
The set of linear equations may be written in matrix form for energy equation as follows;

$$\begin{vmatrix} \beta_1^{/(I)} & \Omega_1^{/(I)} & & & & & & \\ \alpha_2^{/(I)} & \beta_2^{/(I)} & \Omega_2^{/(I)} & & & & & \\ & \alpha_3^{/(I)} & \beta_3^{/(I)} & \Omega_3^{/(I)} & & & & \\ & & - & - & - & & & \\ & & & - & - & - & & \\ & & & & - & - & - & \\ & & & & & \alpha_{n-1}^{/(I)} & \beta_{n-1}^{/(I)} & \Omega_{n-1}^{/(I)} \\ & & & & & & \alpha_n^{/(I)} & \beta_n^{/(I)} \end{vmatrix} \times \begin{vmatrix} \theta_{j+1,1}^{(i+1)} \\ \theta_{j+1,2}^{(i+1)} \\ \theta_{j+1,3}^{(i+1)} \\ - \\ - \\ - \\ \theta_{j+1,n-1}^{(i+1)} \\ \theta_{j+1,n}^{(i+1)} \end{vmatrix} = \begin{vmatrix} \Phi_1^{(I)} - \alpha_1^{/(I)} \\ \Phi_2^{/(I)} \\ \Phi_3^{/(I)} \\ - \\ - \\ - \\ \Phi_{n-1}^{/(I)} \\ \Phi_n^{/(I)} \end{vmatrix} \quad (18)$$

Where

$$\alpha_k^{/(I)} = -\frac{1}{(\mathrm{Pr})(\Delta Y)^2} - \frac{V_{j+1,k}^{(I+1)}}{2(\Delta Y)} \qquad \beta_k^{/(I)} = \frac{2}{(\mathrm{Pr})(\Delta Y)^2} + \frac{U_{j+1,k}^{(I+1)}}{\Delta X}$$

$$\Phi_k^{/(I)} = \frac{U_{j+1,k}^{(I+1)}.\theta_{j,k}}{\Delta X} \qquad \Omega_k^{/(I)} = -\frac{1}{(\mathrm{Pr})(\Delta Y)^2} + \frac{V_{j+1,k}^{(I+1)}}{2(\Delta Y)}$$

Dimensionless Local And Average Nusselt Number

The local Nusselt number in dimensionless form is given by;

$$Nu_x = \left.\frac{\partial\theta}{\partial Y}\right|_{Y=0} (X)(Gr) \quad (19)$$

In finite difference form this equation can be written as;

$$Nu_x = \left[\frac{3\theta_{j+i,0} - 4\theta_{j+1,1} + \theta_{j+1,2}}{}\right](X)(Gr) \quad (20)$$

The average Nusselt number is given by;

$$Nu_m = \frac{1}{X}\int_0^X Nu_x.dx \quad (21)$$

Results And Discussion

The layout of results include three values for Grashoff number are selected (5,10, & 100) and two values for Prandtl number are selected (0.71,7). The thermal boundary condition for this problem is constant wall temperature. These results includes the dimensionless velocity in X and Y directions respectively (U,V) & dimensionless temperature distribution (θ). **Figures (2 to 4)** show the velocity profiles in the axial direction of the plate. It can be seen from these **figures** that initial velocity equal zero when X=0, then it increases gradually as x increases yielding to maximum values of U between surface and hydrodynamic boundary layer and theses maximum values are closer to wall than to surroundings. Its observed that the increase in Grashoff numbers yields to increase in axial velocity, positive values are selected since the temperature of the plate is less than surrounding temperature. The values of Grashoff number are selected closed together in order to

make good comparison between the present work and the available models presented in the literature. **Figures (5 to 7)** represent the effect of Gr on the velocity profile in the horizontal direction. It's observed that all values of V have negative values since positive values of Gr means the plate is cooled from he surroundings ($T_{plate} < T\infty$). **Figures (8 to 13)** shows the temperature distribution along the plate. It's noted that the increase in the Pr valued result in decrease in the temperature distribution. The reason is that smaller values of Prandtl number are equivalent to increasing thermal conductivity and therefore heat is able to diffuse away from the cooled surface more rapidly than for higher values of Pr, **Spalding, 1980.** Increase in the Gr number yields ton increase in velocity which in turn increases the temperature distribution. **Figures (14)** shows the axial development of local Nusselt number along the plate, Nusselt number has the maximum value at the start of plate (first step) and then decreases gradually. The boundary layer thickness is zero at the start of plate , hence, there is no resistance against heat transfer which leads to raise the heat transfer coefficient value to maximum.

Conclusion

The following conclusions are drawn from this study; the procedure adapted not need to assume any initial values that means the matrix is built, and then it solved using **Gauss- Elimination method**. All velocities in the horizontal direction of the plate have negative values indicates that the plate is cooled by the medium, so positive values for the Grashoff number are selected. More heat is exchanged when Prandtl number is increased. The thickness of the thermal boundary layer for air (Pr=0.71) is greater than for water, (Pr=7), and there is more uniform temperature distribution across the thermal boundary layer for air as compared for water.

Model Verfication

Figures (15) & (16) show a comparison between present model and the models predicted by **Holman, 1999** and **Spalding, 1980** Models respectively. It can be seen that the agreement between these results is fairly encouraging, and the trends of shape changes are also quite as anticipated. **Fig.(15),&(16)** indicate that there are reasonable agreements between this work and these models and imply that present work is regarded as a potentially useful tool for predicting the velocity profile and temperature distribution.

References

Amable y Kurdyumov, V. "Laminar free convection induced by a line heat source and heat transfer from wires at small Grashof numbers." Journal of Fluid Mechanics. vol. 362, pp. (199-227), 1998.

Anderson, D.A., Tannehill, J.C., and Pletcher, R.H., "Computational Fluid Mechanics and Heat Transfer", McGraw-Hill Book Company, New York, 1984.

Ayo S.A.," Transient Free Convection Generated by a Heated Vertical Plate in a Rectangular Cavity**"**
AU J.T. Vol.10, No.1, pp (55-62), 2006.

Beithou N. AL-bayrak K., Abdul majeed A.," Effects of Porosity on the Free Convection Flow of Non-Newtonian Fluids Along a Vertical Plate Embedded in a Porous Medium", Tr. J. of Engineering and Environmental Science, 1998.

Chaudhary R.C., Preeti Jain, "Unsteady Free Convection Boundary-Layer Flow Past An Impulsively Started Vertical Surface with Newtonian Heating", Rom. Journ. Phys., Vol. 51, No. 9–10, pp.(911–925), Bucharest, 2006

Grae Worster and Alison Leitch," Laminar free convection in confined regions", Journal of Fluid Mechanics Digital Archive, **156** , pp (301-319), 1985.

Holman, J.P., "Heat Transfer", McGraw-Hill Book Company, New York, 1999.

Hornbeck, R.W., "Numerical Marching Techniques for Fluid Flows with Heat Transfer", National Aeronautics and Space Administration, Washington, 1973.

Incropera, F.P. and Dewitt, D.P., "Fundamentals of Heat and Mass Transfer", John Wiley & Sons, New York, 1996.

Schlichting, H., "Boundary-Layer Theory", McGraw-Hill Book Company, New York, 1968.

Spalding, D.B. "Natural convection heat and mass transfer", Volume 5, 1980.

Table (1): Average Nusselt number

		Gr		
		5	10	100
Pr	0.71	1.386	1.52	2.173
	7	2.169	2.45	3.83

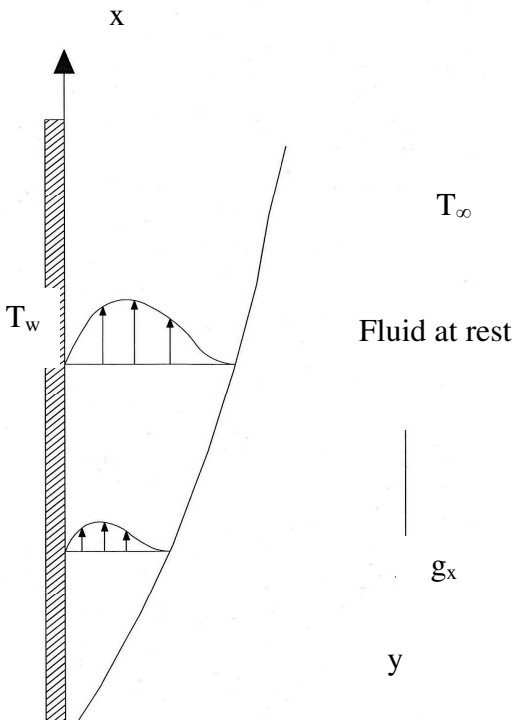

Figure (1) Physical Model and Its Coordinates System

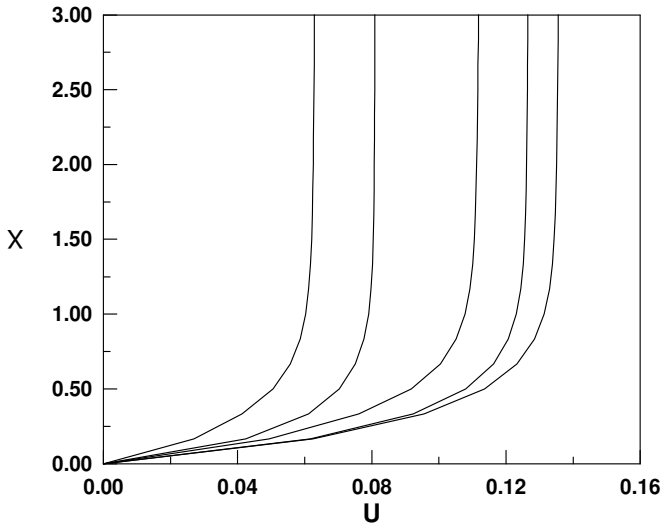

Figure(2) Velocity profile in the axial direction of the plate (Gr=5)

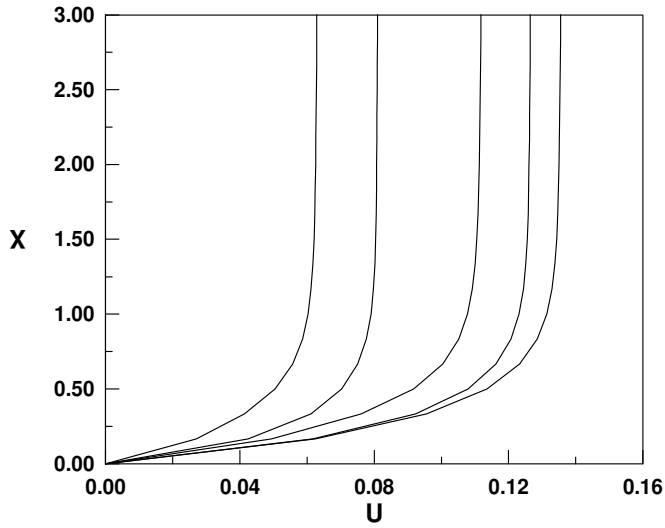

Figure (3) Velocity profile in the axial direction of the plate (Gr=10)

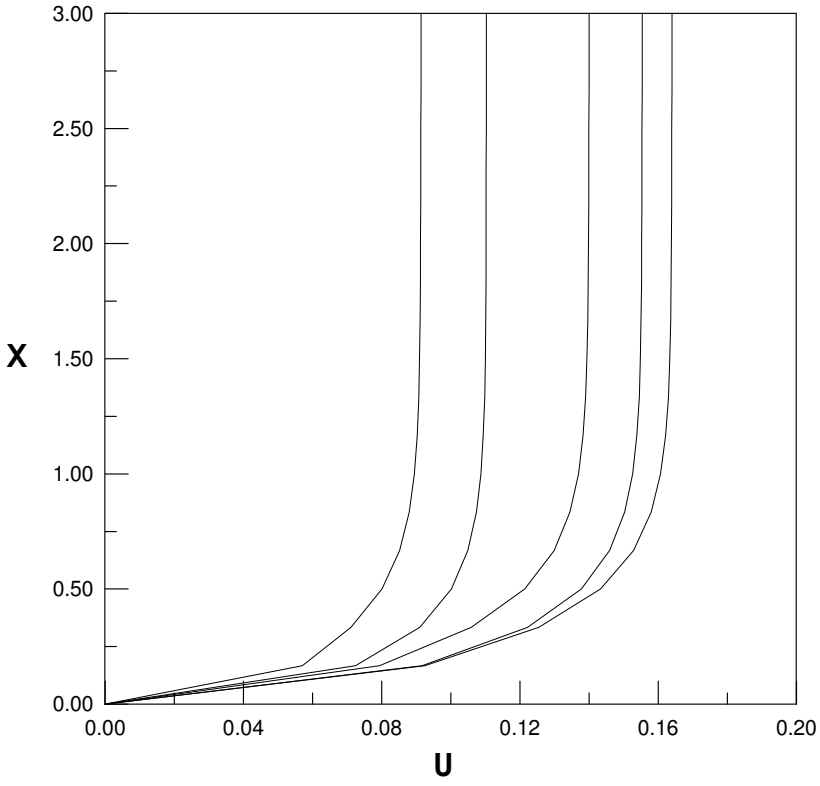

Figure (4) Velocity profile in the axial direction of the plate (Gr=100)

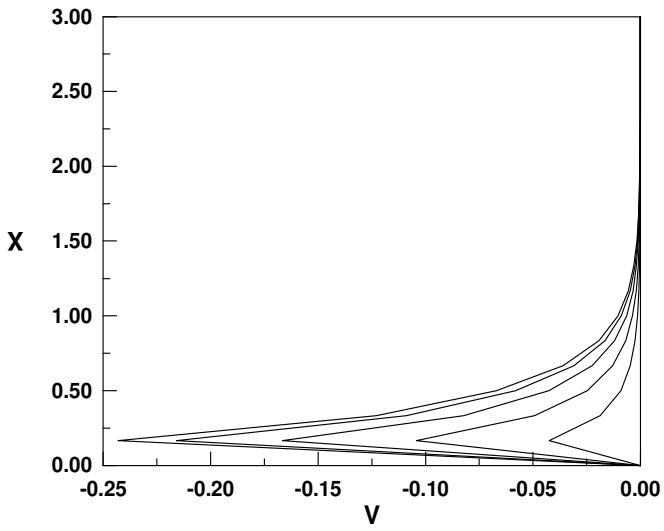

Figure (5) Velocity profile in the vertical direction of the plate (Gr=5)

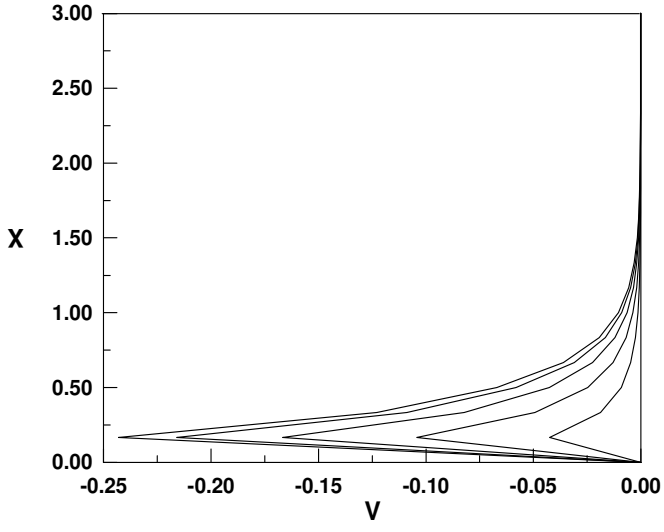

Figure (6) Velocity profile in the vertical direction of the plate (Gr=10)

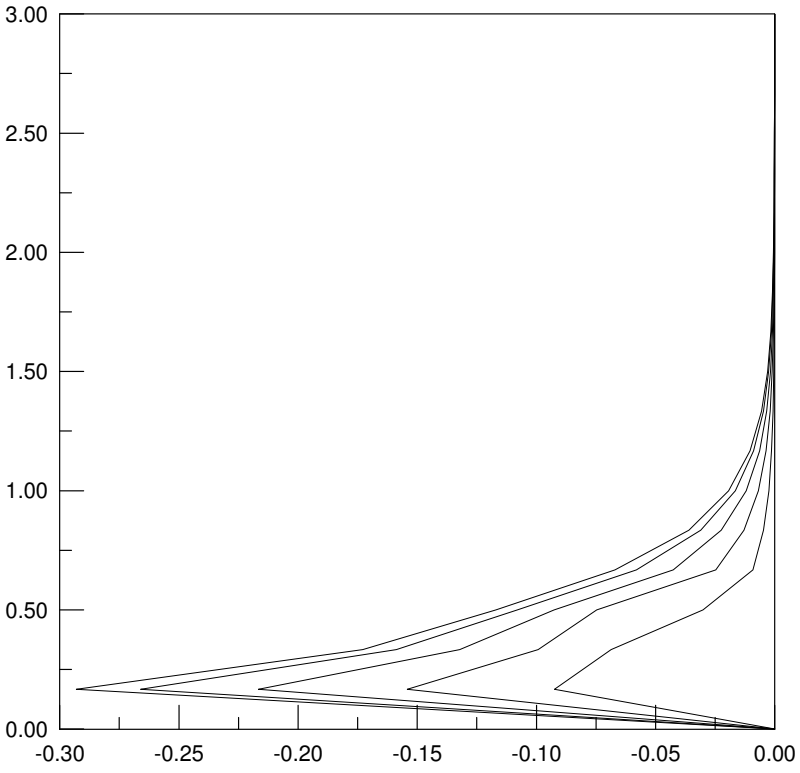

Figure (7) Velocity profile in the vertical direction of the plate (Gr=100)

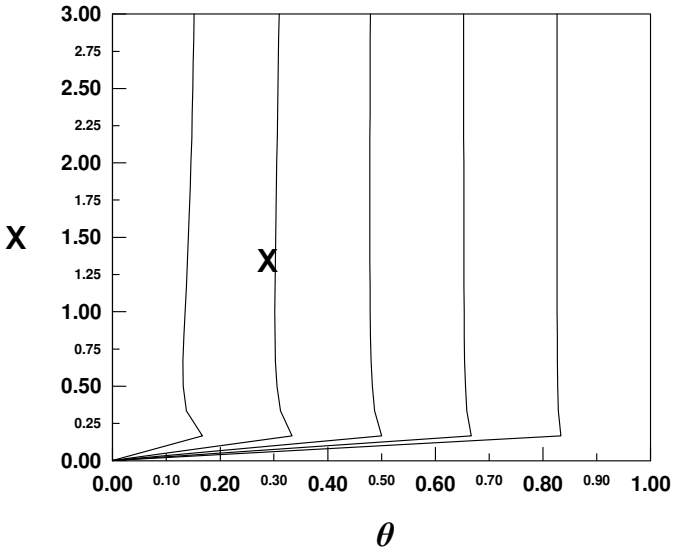

Figure(8) Temperature Distribution in the axial direction of the plate (Pr=0.71, Gr=5)

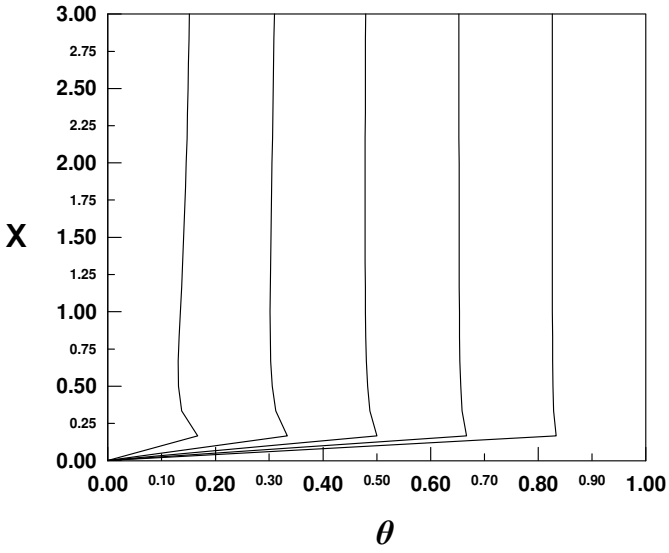

Figure (9) Temperature Distribution in the axial direction of the plate (Pr=0.71, Gr=10)

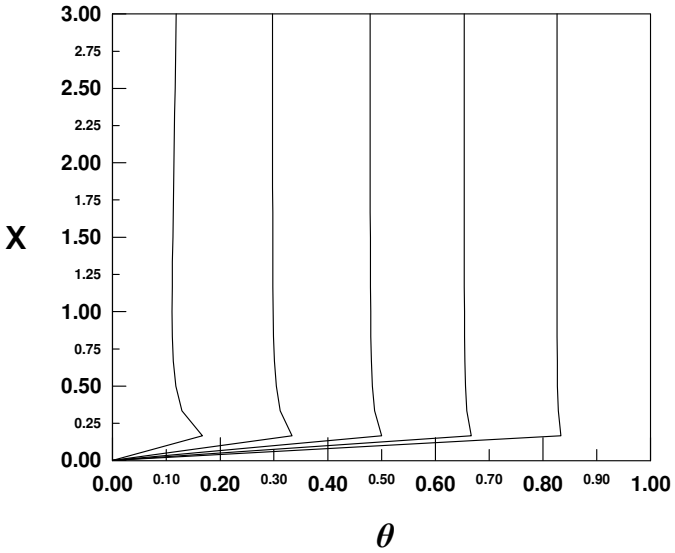

Figure (10) Temperature Distribution in the axial direction of the plate (Pr=7, Gr=5)

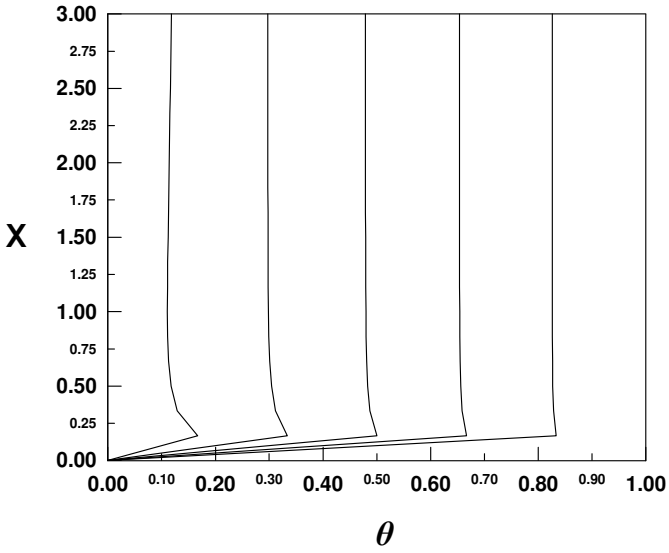

Figure (11) Temperature Distribution in the axial direction of the plate (Pr=7, Gr=10)

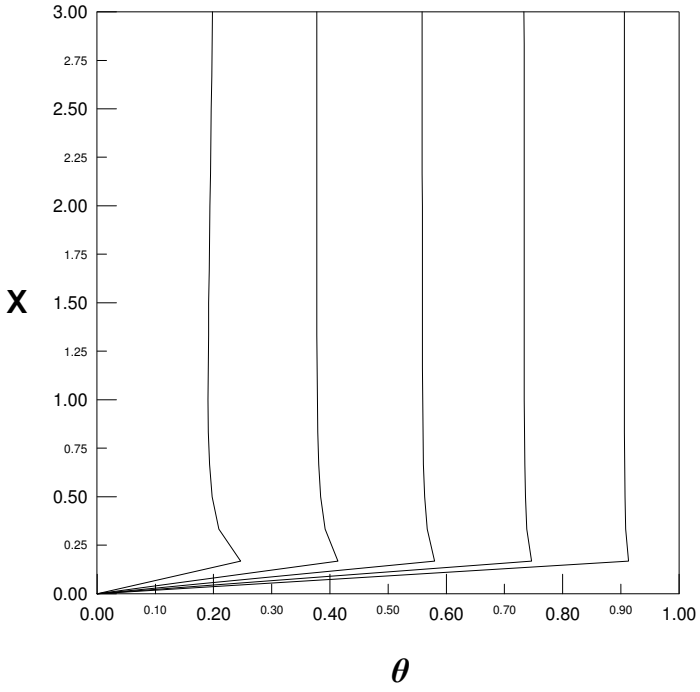

Figure (12) Temperature Distribution in the axial direction of the plate (Pr=0.71, Gr=100)

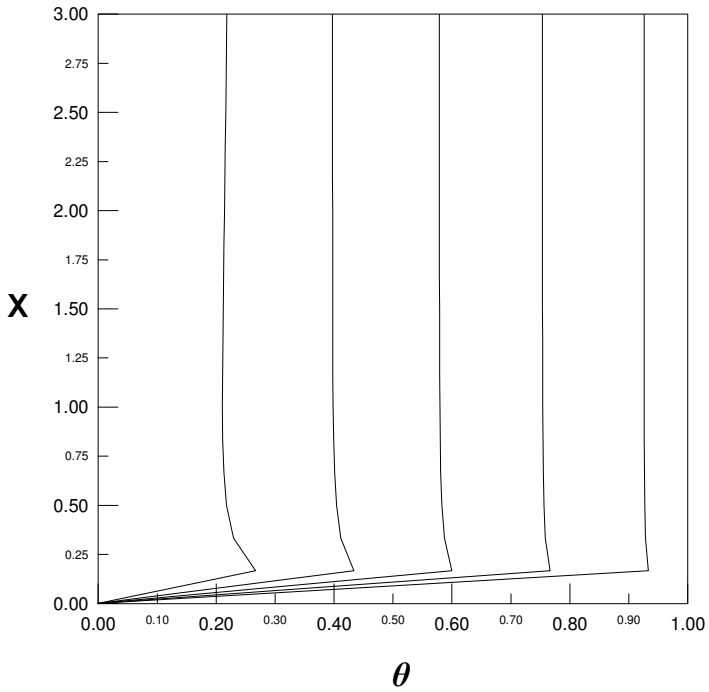

Figure (13) Temperature Distribution in the axial direction of the plate (Pr=7, Gr=100)

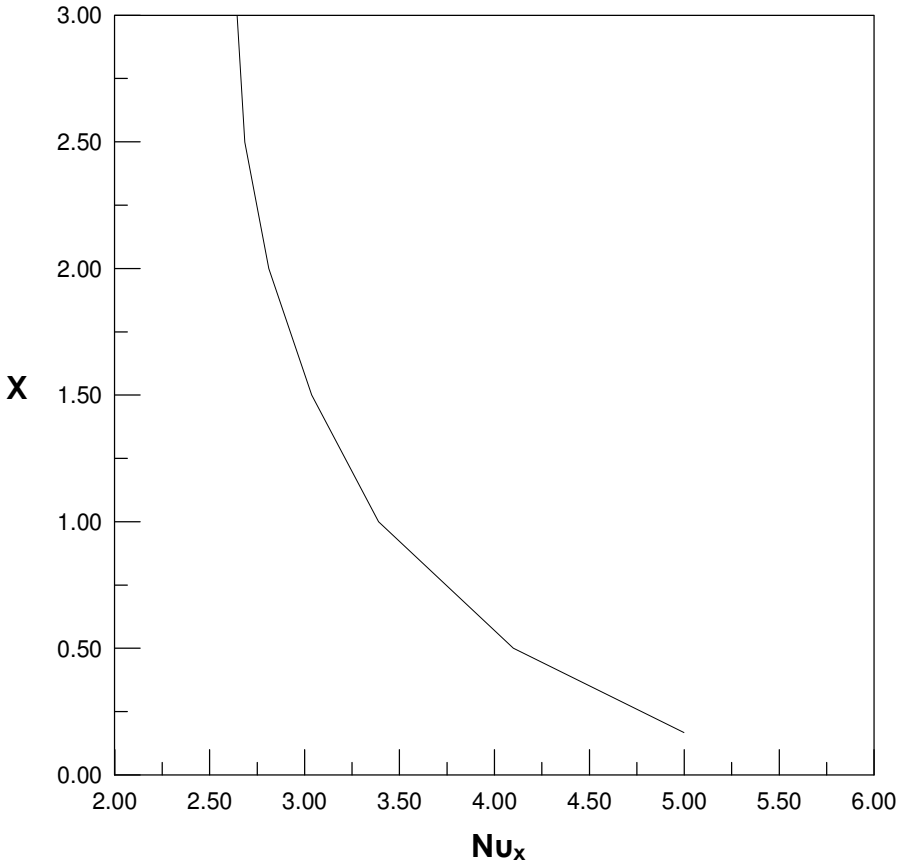

Figure (14) Local Nusselt number in the axial direction of the plate (Pr=7, Gr=100)

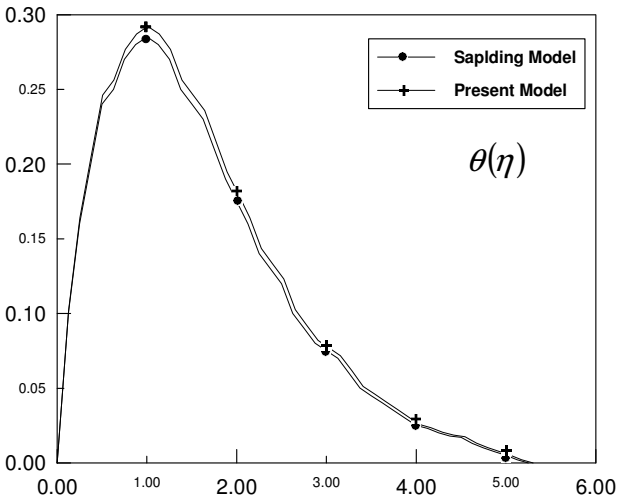

$$\eta = \frac{y}{x}\left(\frac{Gr_x}{4}\right)^{1/4}$$

Figure (15) Velocity variation across boundary layer, a comparison between Present model and Spalding model

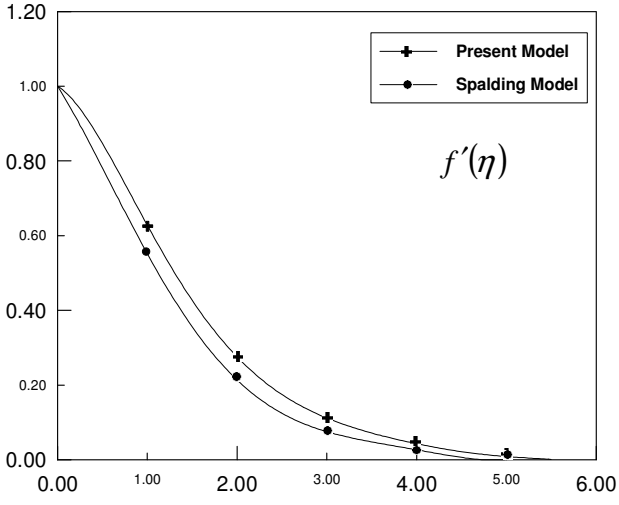

$$\eta = \frac{y}{x}\left(\frac{Gr_x}{4}\right)^{1/4}$$

Figure (16) Temperature variation across boundary layer, a comparison between Present model and Spalding model

$$\theta(\eta) = \frac{T - T_\infty}{T_w - T_\infty}$$

$$f'(\eta) = \frac{V_x x}{2v\sqrt{Gr_x}}$$